Journal Name

COMMUNICATION

Assembling metallic 1T-MoS₂ nanosheets with inorganic-ligand stabilized quantum dots for exceptional solar hydrogen evolution

Xu-Bing Li, Yu-Ji Gao, Hao-Lin Wu, Yang Wang, Qing Guo, Mao-Yong Huang, Bin Chen, Chen-Ho Tung and Li-Zhu Wu*

Due to enhanced light harvesting, favored interfacial charge transfer and excellent proton reduction activity, the hybrid photocatalysts of metallic 1T-MoS₂ nanosheets and inorganic-ligand stabilized CdSe/ZnS QDs obtained *via* a self-aasembled approach can produce H₂ gas with a rate of ~155 ± 3.5 μmol^{-1} h^{-1} mg^{-1} under visible-light irradiation (λ = 410 nm), an exceptional performance of solar H₂ evolution using MoS₂ as cocatalysts known to date.

Water splitting is regarded as a promising avenue to achieve solar-to-fuel conversion *via* photocatalytic hydrogen (H₂) evolution.[1] In this regard, platinum has shown excellent electrocatalytic and photocatalytic activities toward H₂ evolution. Unfortunately, the high cost and scarcity limit its large-scale application. Therefore, development of earth-abundant, low-cost and high-efficient cocatalysts to realize sustainable and large-scale H₂ production is in its great necessity. MoS₂, evidenced by experimental and theoretical results, is a very promising candidate for both electro- and photo-catalytic H₂ evolution.[2] Due to the extremely large edge-site exposure, excellent electronic conductivity and abundant new formed trap states and vacancies, metallic 1T-MoS₂ nanosheets have attracted special attention in recent years for electrocatalytic H₂ production than the state-of-the-art forms of MoS₂.[3]

Unlike electrocatalytic H₂ evolution, the use of 1T-MoS₂ nanosheets for photocatalytic H₂ production is in its infancy.[4] For establishing a high-efficient photocatalytic H₂ evolution system using 1T-MoS₂ nanosheets, the following aspects should be achieved: (1) excellent visible-light response and exciton generation of the light absorbers are required; (2) intact coupling between light absorbers and two-dimensional 1T-MoS₂ nanosheets is preferred; and (3) the energy barrier of

interfacial electron transfer from light absorbers to the two-dimensional nanosheets should be greatly reduced. Among various light absorbers, colloidal semiconductor quantum dots (QDs) are regarded as the ideal candidate due to their predominant advantages in visible-light harvesting, multi-exciton generation, charge separation, and easy to surface modification.[5] Furthermore, modification of QDs with metal-free inorganic ligands, such as chalcogenide anions, can greatly reduce the energy barrier of interfacial charge transport, which would provide advantages for enhanced solar H₂ production.[6] Therefore, coupling 1T-MoS₂ nanosheets with all-inorganic QDs would be a promising approach to achieve high efficiency of solar-to-fuel conversion *via* solar H₂ evolution.

In the present work, we, for the first time, couple metallic 1T-MoS₂ nanosheets with all-inorganic CdSe/ZnS QDs for solar H₂ evolution *via* a self-assembled approach. Under the optimal conditions (λ = 410 nm), the rate of H₂ evolution was estimated to be ~155 ± 3.5 μmol^{-1} h^{-1} mg^{-1}, which is an exceptional performance of solar H₂ evolution using MoS₂ as the cocatalyst. Experimental evidence indicates that the extremely high activity of solar H₂ production arises from the synergistic effect of the enhanced light absorbing and exciton generation of CdSe/ZnS QDs, the reduced energy barrier of interfacial charge transfer and also the abundant active sites for proton reduction of 1T-MoS₂ nanosheets. In virtue of these advantages, the self-assembled photocatalysts show excellent activity towards solar H₂ evolution.
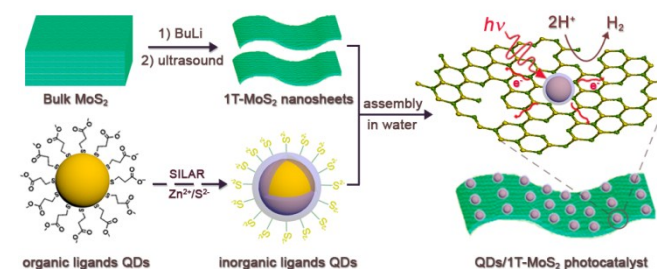
Scheme 1 Schematic illustration of the fabrication of QDs/1T-MoS₂ photocatalysts *via* a self-assembled approach.
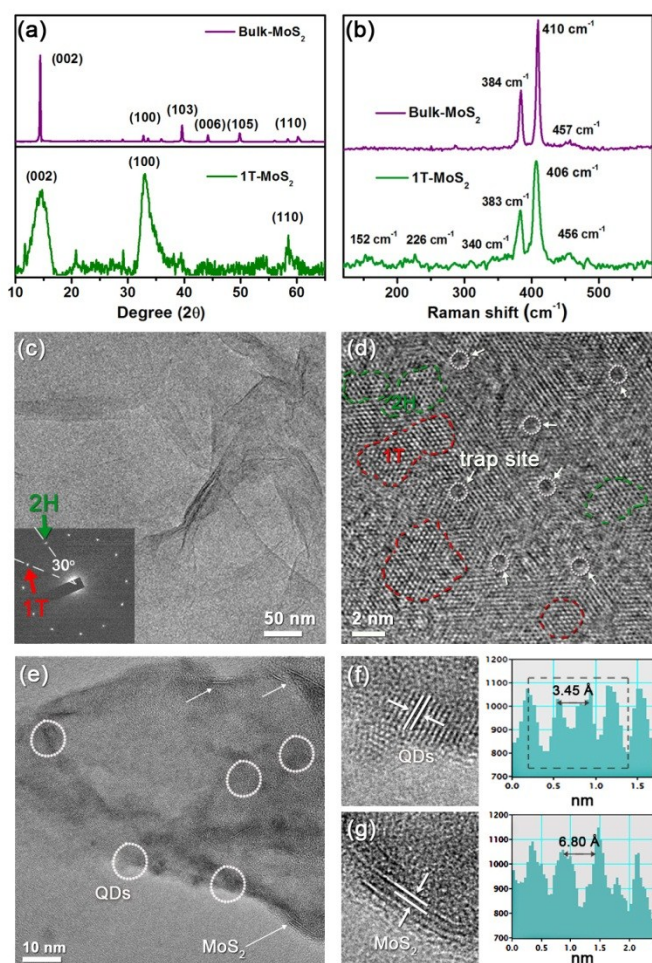
Fig. 1 (a) XRD patterns and (b) Raman spectra of bulk 2H-MoS$_2$ and 1T-MoS$_2$ nanosheets; (c) TEM image of 1T-MoS$_2$ nanosheets (inset is the corresponding SAED); (d) High-resolution TEM image of the obtained 1T-MoS$_2$ nanosheets; (e) TEM characterization of QDs/1T-MoS$_2$ photocatalysts; (f) high-resolution TEM of QDs in (e) and the corresponding lattice distance of (111) plane; (g) high-resolution TEM of MoS$_2$ in (e) and the corresponding lattice fringe of (002) plane.

The composite photocatalysts of QDs/1T-MoS$_2$ were prepared through a self-assembled process, as shown in Scheme 1. Metallic 1T-MoS$_2$ nanosheets were obtained *via* lithium intercalation of bulk-MoS$_2$ for one week at room temperature, see details in supporting information. The dramatically diminished intensity of (002) peak of bulk MoS$_2$ in X-ray diffraction (XRD) pattern indicated the destruction of long-range stacking of the layered structure into exfoliated nanosheets (Fig. 1a). The broadening of all peaks showed poor crystallinity of the obtained materials. The decreased intensity of Raman peaks at 410 cm^{-1} and 384 cm^{-1} also indicated the destruction of layered packing structure of bulk MoS$_2$. Besides, the emergence of new Raman shifts at 152 cm^{-1}, 226 cm^{-1} and 340 cm^{-1} could be ascribed to phonon modes of 1T-MoS$_2$, confirming the transformation of bulk 2H-MoS$_2$ to 1T-MoS$_2$ counterparts (Fig. 1b). Transmission electron microscopy (TEM) verified the ultrathin nature of the as-prepared 1T-MoS$_2$ samples (Fig. 1c). Selected area electron diffraction (SAED)

pattern in the inset panel of Fig. 1c showed a typical hexagonal spot pattern corresponding to 2H-MoS$_2$. The extra strong hexagonal spot at 30° between the hexagonal spots could be assigned to 1T-MoS$_2$.[4] The coexistence of 1T-MoS$_2$, the regions in red circles, and 2H-MoS$_2$, the regions in green circles, could be further evidenced by high-resolution TEM image in Fig. 1d. Also, abundant trap sites were directly observed in TEM image as denoted by the white arrows in Fig. 1d, indicating the abundant active sites. All inorganic CdSe/ZnS QDs were obtained by a modified successive ionic layer adsorption and reaction method of growing ZnS shell on the surface CdSe cores, see detailed characterizations in Fig. S1-S3. Because of the strong electrostatic attraction between negatively charged QDs and positively charges MoS$_2$ nanosheets and the coordination of sulfur with molybdenum,[7] CdSe/ZnS QDs could spontaneously assemble with 1T-MoS$_2$ nanosheets to form composite photocatalysts in aqueous solution. TEM image in Fig. 1e directly verified the successfully loading of QDs on the surface of 1T-MoS$_2$ nanosheets. The enlarged TEM images showed lattice fringes of about 3.45 Å (Fig. 1f) and 6.80 Å (Fig. 1g), which could be ascribed to the (111) plane of QDs and (002) plane of MoS$_2$ respectively, directly confirming the QDs on 1T-MoS$_2$ nanosheets.
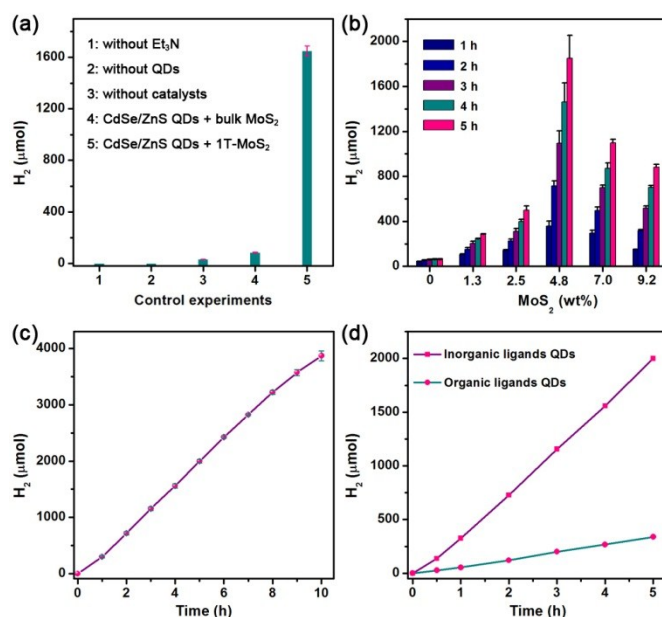
Fig. 2 (a) Control experiments of visible-light-induced H$_2$ evolution in 5.0 h (λ = 410 nm); (b) the variation of solar H$_2$ evolution with different weight ratios of MoS$_2$; (c) solar H$_2$ evolution under the optimal conditions; (d) the influence of surface ligands on H$_2$ production. Error bars represent mean $\pm$ s.d. of at least three independent experiments.

The initial photocatalytic H$_2$ evolution performance of the obtained photocatalysts was examined using triethylamine (Et$_3$N) as sacrificial reagent under visible-light irradiation (λ = 410 nm). As presented in Fig. 2a, the assembled photocatalysts of CdSe/ZnS QDs and 1T-MoS$_2$ nanosheets could produce ~1650 ± 40 μmol molecular H$_2$ in 5.0 hour, which was almost 20-fold to that of CdSe/ZnS QDs and bulk MoS$_2$ (84 ± 3.0 μmol)

under identical condition. Control experiments indicated that QDs, 1T-MoS$_2$ nanosheets and sacrificial reagent were all necessary for efficient photocatalytic H$_2$ evolution (Fig. S4). The effect of weight percentage of 1T-MoS$_2$ nanosheets on the rate of H$_2$ production was carefully investigated. As shown in Fig. 2b, progressive increase of the weight percentage of 1T-MoS$_2$ from o to 4.8 wt% significantly improved the activity of photocatalytic H$_2$ production. However, further increasing the weight percentage of 1T-MoS$_2$ reduced the rate of H$_2$ evolution, which was due to the light-screening effect of excessive amount of cocatalysts. Under the optimal conditions, the assembled photocatalysts of inorganic-ligand stabilized CdSe/ZnS QDs and 1T-MoS$_2$ nanosheets could evolve H$_2$ gas with a constant rate of ~156 ± 3.5 $\mu mol^{-1} h^{-1} mg^{-1}$ during 10 h irradiation (Fig. 2c). The photocatalytic activity significantly declined after a long-time irradiation. With addition of extra amount of sacrificial reagent into the system, the activity of solar H$_2$ evolution recovered immediately (Fig. S5). The similar rate of H$_2$ evolution with that of the initial stage indicated the depletion of electron donor was the major reason of declined H$_2$ production activity.
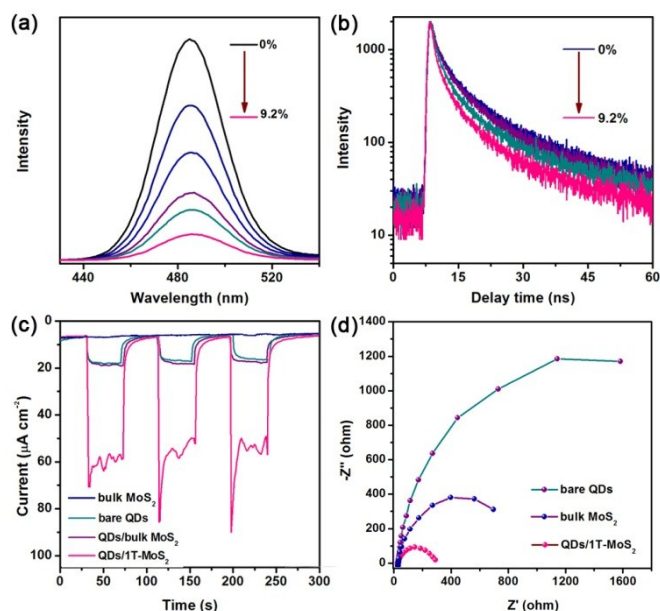
Fig. 3 (a) Steady-state emission quenching and (b) corresponding lifetime decay of QDs by coupling with different amounts of 1T-MoS$_2$ nanosheets; (c) transient photocurrent responses of bulk MoS$_2$, bare CdSe/ZnS QDs, CdSe/ZnS QDs/1T-MoS$_2$ (4.8 wt%) and CdSe/ZnS QDs/bulk MoS$_2$ (4.8 wt%) electrodes to on-off illumination (λ > 400 nm); (d) electrochemical impedance spectroscopy Nyquist plots of bare QDs, bulk MoS$_2$ and CdSe/ZnS QDs/1T-MoS$_2$ (4.8 wt%) electrodes.

In order to reveal the intrinsic reasons of the exceptional photocatalytic H$_2$ evolution performance of this system, various experiments have been performed. As shown in Fig. S6, the obtained CdSe/ZnS QDs acquired much better light response in the realm of visible-light region. Compared with CdSe core, the band-edge emission of CdSe/ZnS QDs was dramatically enhanced along with the decrease of trap-state emission, which would inhibit exciton trapping at trap states

(Fig. S7). As shown in Fig. 3a, the emission intensity of CdSe/ZnS QDs was dramatically quenched by coupling with 1T-MoS$_2$ nanosheets, suggesting that the recombination of photogenerated electron-hole pairs was efficiently inhibited. Also, the emission lifetime of CdSe/ZnS QDs decayed from ~20 to ~9.0 ns upon assembling with 1T-MoS$_2$ nanosheets (Fig. 3b), indicating the well interfacial electron transfer from QDs to 1T-MoS$_2$ nanosheets.

Photoelectrochemical measurements provided more information on the process of facile interfacial charge transfer. As shown in Fig. 3c, the photocurrent transient responses of QDs/1T-MoS$_2$ (4.8 wt%) electrode were much higher than those of QDs, bulk MoS$_2$ and QDs/bulk MoS$_2$ counterparts under the same conditions. The much smaller arc radius of electrochemical impedance spectroscopy (EIS) Nyquist plot of QDs/1T-MoS$_2$ (4.8 wt%) electrode than those of bare QDs and bulk MoS$_2$ implied the faster interfacial electron transfer (Fig. 3d). The favored interfacial electron transfer from inorganic-ligand stabilized QDs to cocatalysts of 1T-MoS$_2$ was also directly confirmed by solar H$_2$ evolution experiments, as shown in Fig. 2d. When the surface ligands of CdSe/ZnS QDs were replaced by organic counterparts, such as 3-mercaptopropionic acid, the rate of photocatalytic H$_2$ evolution decreased to ~68 $\mu mol\ h^{-1}$, which was only one sixth of the inorganic ligands stabilized counterparts (~400 $\mu mol\ h^{-1}$) under identical conditions.

Besides, the abundant trap states and edge sites of the obtained 1T-MoS$_2$ contributed a lot to the remarkable solar H$_2$ production performance. It had been reported that both S-vacancy and Mo-edge of MoS$_2$ demonstrated an close-to-zero Gibbs free energy change,[8] thus promoting the processes of proton adsorption and reduction at active sites of 1T-MoS$_2$ nanosheets (Fig. S8). Taken all together, we can conclude that the enhanced visible-light response, the facilitated interfacial charge transfer, and the excellent proton reduction ability of metallic 1T-MoS$_2$ nanosheets enable this system to show exceptional activity of solar H$_2$ evolution.

In summary, we have firstly coupled 1T-MoS$_2$ nanosheets with inorganic-ligands stabilized CdSe/ZnS QDs *via* a self-assembling approach for solar-to-fuel conversion application. The obtained assembled photocatalysts is able to evolve H$_2$ gas with a rate of ~155 ± 3.5 $\mu mol^{-1} h^{-1} mg^{-1}$ under the optimum conditions. The unprecedented activity of solar H$_2$ evolution is a result of enhanced light harvesting, the facilitated interfacial charge transfer and excellent proton reduction ability of vacancy-rich 1T-MoS$_2$ nanosheets. It is anticipated that this research line can lead to the fabrication of smarter, cheaper and more robust artificial photocatalysts for solar H$_2$ evolution, which is actively undergoing in our research group.

Notes and references

1　(a) W. Wang, J. Chen, C. Li and W. Tian, *Nat Commun*, 2014, **5**, 4647; (b) W. Bi, X. Li, L. Zhang, T. Jin, L. Zhang, Q. Zhang, Y. Luo, C. Wu and Y. Xie, *Nat Commun*, 2015, **6**, 8647; (c)　L.-Z.　Wu,　B. Chen, Z.-J. Li and C.-H. Tung, *Acc. Chem. Res.*, 2014, **47**, 2177-2185; (d) J. Barber, *Chem. Soc. Rev.*, 2009, **38**, 185-196; (e) S. Berardi, S. Drouet, L. Francas, C. Gimbert-Surinach, M. Guttentag, C. Richmond, T. Stoll and A. Llobet, *Chem. Soc. Rev.*, 2014, **43**, 7501-7519; (f)　　V. Artero, M. Chavarot-Kerlidou and M. Fontecave, *Angew. Chem. Int. Ed.*, 2011, **50**, 7238-7266; (g) Y. Zheng, Y. Jiao, M. Jaroniec and S. Z. Qiao, *Angew. Chem. Int. Ed.*, 2015, **54**, 52-65; (h) X.-B. Li, Y.-J. Gao, Y. Wang, F. Zhan, X.-Y. Zhang, Q. Kong, N.-J. Zhao, Q. Guo, H.-L. Wu, Z.-J. Li, Y. Tao, J.-P. Zhang, B. Chen, C.-H. Tung and L.-Z. Wu, *J. Am. Chem. Soc.*, 2017, **139**, 4789-4796; (i) K. Maeda, M. Higashi, D. Lu, R. Abe and K. Domen, *J. Am. Chem. Soc.*, 2010, **132**, 5858-5868; (j) K. Maeda, *ACS Catal.*, 2013, **3**, 1486-1503; (k) S. Wang, W. Yao, J. Lin, Z. Ding and X. Wang, *Angew. Chem. Int. Ed.*, 2014, **53**, 1034-1038; (l) S. Wang and X. Wang, *Angew. Chem. Int. Ed.*, 2016, **55**, 2308-2320.

2　(a) X. Zong, H. Yan, G. Wu, G. Ma, F. Wen, L. Wang and C. Li, *J. Am. Chem. Soc.*, 2008, **130**, 7176-7177; (b) T. F. Jaramillo, K. P. Jørgensen, J. Bonde, J. H. Nielsen, S. Horch and I. Chorkendorff, *Science*, 2007, **317**, 100-102; (c) X. Zong, Y. Na, F. Wen, G. Ma, J. Yang, D. Wang, Y. Ma, M. Wang, L. Sun and C. Li, *Chem. Commun.*, 2009, **30**, 4536-4538; (d) M. Liu, F. Li, Z. Sun, L. Ma, L. Xu and Y. Wang, *Chem. Commun.*, 2014, **50**, 11004-11007; (e) Y. Yin, J. Han, Y. Zhang, X. Zhang, P. Xu, Q. Yuan, L. Samad, X. Wang, Y. Wang, Z. Zhang, P. Zhang, X. Cao, B. Song and S. Jin, *J. Am. Chem. Soc.*, 2016, **138**, 7965-7972; (f) J. Xie, H. Zhang, S. Li, R. Wang, X. Sun, M. Zhou, J. Zhou, X. W. Lou and Y. Xie, *Adv. Mater.*, 2013, **25**, 5807-5813; (g) T. Wang, L. Liu, Z. Zhu, P. Papakonstantinou, J. Hu, H. Liu and M. Li, *Energy Environ. Sci.*, 2013, **6**, 625-633; (h) Y. Yan, B. Xia, X. Qi, H. Wang, R. Xu, J.-Y. Wang, H. Zhang and X. Wang, *Chem. Commun.*, 2013, **49**, 4884-4886; (i) Y. Hou, A. B. Laursen, J. Zhang, G. Zhang, Y. Zhu, X. Wang, S. Dahl and I. Chorkendorff, *Angew. Chem. Int. Ed.*, 2013, **52**, 3621-3625; (j) Y.-J. Yuan, J.-R. Tu, Z.-J. Ye, D.-Q. Chen, B. Hu, Y.-W. Huang, T.-T. Chen, D.-P. Cao, Z.-T. Yu and Z.-G. Zou, *Appl. Catal., B*, 2016, **188**, 13-22; (k) Y.-J. Yuan, Z.-J. Ye, H.-W. Lu, B. Hu, Y.-H. Li, D.-Q. Chen, J.-S. Zhong, Z.-T. Yu and Z.-G. Zou, *ACS Catal.*, 2016, **6**, 532-541; (l) Z. Kong, Y.-J. Yuan, D. Chen, G. Fang, Y. Yang, S. Yang and D. Cao, *Dalton Trans.*, 2017, **46**, 2072-2076.

3　(a) M. A. Lukowski, A. S. Daniel, F. Meng, A. Forticaux, L. Li and S. Jin, *J. Am. Chem. Soc.*, 2013, **135**, 10274-10277; (b) H. Li, C. Tsai, A. L. Koh, L. Cai, A. W. Contryman, A. H. Fragapane, J. Zhao, H. S. Han, H. C. Manoharan, F. Abild-Pedersen, J. K. Norskov and X. Zheng, *Nat. Mater.*, 2016, **15**, 48-53; (c) Q. Ding, F. Meng, C. R. English, M. Cabán-Acevedo, M. J. Shearer, D. Liang, A. S. Daniel, R. J. Hamers and S. Jin, *J. Am. Chem. Soc.*, 2014, **136**, 8504-8507.

4　(a) U. Maitra, U. Gupta, M. De, R. Datta, A. Govindaraj and C. N. R. Rao, *Angew. Chem. Int. Ed.*, 2013, **52**, 13057-13061; (b) K. Chang, X. Hai, H. Pang, H. Zhang, L. Shi, G. Liu, H. Liu, G. Zhao, M. Li and J. Ye, *Adv. Mater.*, 2016, **28**, 10033-10041.

5　(a) H. Zhu, Y. Yang and T. Lian, *Acc. Chem. Res.*, 2012, **46**, 1270-1279; (b) M. A. Holmes, T. K. Townsend and F. E. Osterloh, *Chem. Commun.*, 2012, **48**, 371-373; (c) A. M. Smith and S. Nie, *Acc. Chem. Res.*, 2009, **43**, 190-200; (d) X.-B. Li, Z.-J. Li, Y.-J. Gao, Q.-Y. Meng, S. Yu, R. G. Weiss, C.-H. Tung and L.-Z. Wu, *Angew. Chem. Int. Ed.*, 2014, **53**, 2085-2089.

6　(a) M. A. Boles, D. Ling, T. Hyeon and D. V. Talapin, *Nat. Mater.*, 2016, **15**, 141-153; (b) M. V. Kovalenko, M. Scheele and D. V. Talapin, *Science*, 2009, **324**, 1417-1420; (c) J.-S. Lee, M. V. Kovalenko, J. Huang, D. S. Chung and D. V. Talapin, *Nat Nano*, 2011, **6**, 348-352.

7　(a) F. A. Frame and F. E. Osterloh, *J. Phys. Chem. C*, 2010, **114**, 10628-10633; (b) A. Nag, D. S. Chung, D. S. Dolzhnikov, N. M. Dimitrijevic, S. Chattopadhyay, T. Shibata and D. V. Talapin, *J. Am. Chem. Soc.*, 2012, **134**, 13604-13615;

8　(a) G. Li, D. Zhang, Q. Qiao, Y. Yu, D. Peterson, A. Zafar, R. Kumar, S. Curtarolo, F. Hunte, S. Shannon, Y. Zhu, W. Yang and L. Cao, *J. Am. Chem. Soc.*, 2016, **138**, 16632-16638; (b) K. Qi, S. Yu, Q. Wang, W. Zhang, J. Fan, W. Zheng and X. Cui, *J. Mater. Chem. A*, 2016, **4**, 4025-4031; (c) Q. Tang and D.-E. Jiang, *ACS Catal.*, 2016, **6**, 4953-4961.

TOC

Assembled QDs/1T-MoS₂ photocatalyst